

POWER COUPLER DESIGN FOR THE LUCRECE PROJECT

H. Guler, O. Bouras, W. Kaabi, M. El Khaldi, D. Auguste, J. Bonis,
 Laboratoire de l'Accélérateur Linéaire CNRS/IN2P3 Université Paris-Saclay, Orsay, France

Abstract

The LUCRECE project aims at developing an elementary RF system (cavity, power source, LLRF and controls) suitable for continuous (CW) operation at 1.3 GHz. This effort is made in the framework of the advanced and compact FEL project LUNEX5 (free electron Laser Using a New accelerator for the Exploitation of X-ray radiation of 5th generation), using superconducting linac technology for high repetition rate and multi-user operation (<http://www.lunex5.com>). In this context, based on its large experience on coupler design and RF conditioning, LAL Laboratory is in charge of the design and the fabrication of RF couplers that could operate at up to 15-20 kW in CW mode. For this purpose, couplers based on Cornell 75kW CW couplers (RF power couplers for the CBETA ERL injector) are under consideration and will be adapted to the LUCRECE needs. Electromagnetic simulations and associated thermal heating will be discussed.

INTRODUCTION

The CBETA injector coupler was the first 1.3 GHz input power coupler to operate at relatively high power in CW mode (75 kW). It was designed starting from TTF III double window coupler model [1]. However, it has been significantly modified to fulfil the ERL injector requirements [2]:

- The cold part was completely redesigned using a 62 mm, 60Ω coaxial line (instead of a 40 mm, 70Ω line) for a better power handling, more efficient heat load dissipation and to avoid multipacting.
- The antenna tip was enlarged and shaped for stronger coupling.
- The outer conductor bellows design (both in warm and cold coaxial lines) was improved for better cooling (Heat intercepts were added).
- Forced air-cooling of the warm inner conductor bellows and “warm” ceramic window was added.

The Cornell coupler design was then used in several CW machine like ARIEL at TRIUMF (20kW) [3] or BESSY VSR at HZB (10kW) [4]. The following study aims to adapt the Cornell coupler design to our need in the framework of coupler prototyping for LUNEX5 machine project (20kW in CW mode). RF studies and thermal simulations results for different design configurations will be presented and discussed.

ELECTROMAGNETIC SIMULATIONS

The coupler electromagnetic (EM) behaviour has been simulated using the ANSYS/HFSS software. The mechanical geometry has been simplified, by removing all the unnecessary parts like the screw holes, and all the different sharp edges, that will not contribute to the simulation

of EM wave propagation inside the coupler. The outer geometry complications are also neglected in the simulation since the wave propagation in the conductor is not influenced by the coupler external part. All unnecessary geometric complication would increase the mesh amount and therefore the simulation time. Regarding the coupler design, the simulated electromagnetic RF wave is not symmetric which forbids using axial symmetry to increase the simulation speed. The 3D simulation is then necessary. The wave propagation inside the coupler has been simulated as showed on Fig. 1.

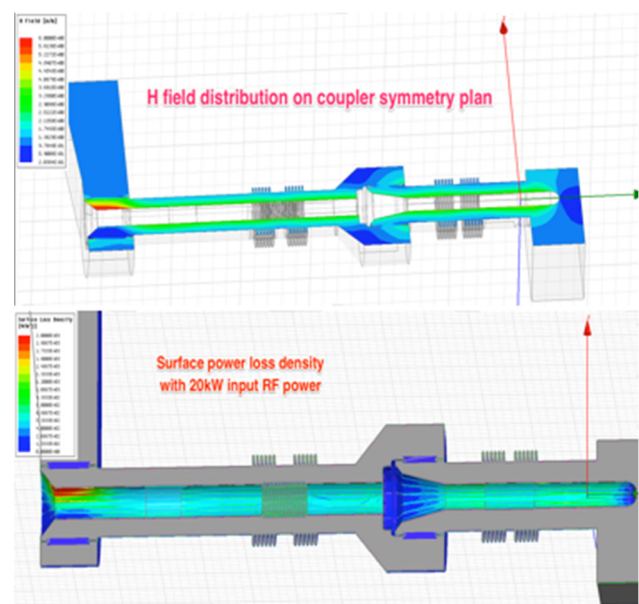


Figure 1: HFSS simulations with the Cornell coupler geometry: H field distribution on the coupler symmetry plan (top) and the surface power loss density on the inner conductor surface (down).

The field distributions shown its highest value in the warm inner conductor in the warm ceramic side where the RF power input is delivered. Deposited RF power has been simulated on the different copper surfaces of the inner conductor, including the bellows that are the area that needed the most accurate meshing. The propagation of RF wave in the coupler generates losses with joule effect in the Inner (CI)/Outer (CX) conductor and dielectric losses in the ceramic windows, as a result, each of these elements will heat up.

The heating in the ceramics has been induced by the EM wave that deposited power inside the ceramics and can be calculated via the following formula:

$$P_{vol} = \epsilon \iint E^2 dV \quad (1)$$

With $\epsilon = \tan(\beta) \approx 1.0 \times 10^{-4}$ for the ceramics. Concerning the ceramics and at 10 kW input power in CW mode,

Content from this work may be used under the terms of the CC BY 3.0 licence (© 2017). Any distribution of this work must maintain attribution to the author(s), title of the work, publisher, and DOI.

the deposited power is few tens of Watt, which will imply temperature rise during RF processing.

Starting from the Cornell coupler design, the geometry has been modified in order to match the 40mm diameter size of the elliptic cavity flange (LCLS2 type). One possible solution proposed is to keep the warm Cornell window as it is, and replace the cold one with an XFEL type 40mm coupler cold window. At low input power, impedance gap (from 60Ω to 70Ω) has negligible effect on the RF behavior. Accurate multipacting simulation must be done before considering any conditioning using pulsed RF signal that could reach 1 MW as for the XFEL coupler conditioning. Over heating could also be increased as respect to the Cornell type cavity principally because of the lower pipe radius in the cold window as shown on Fig. 2.

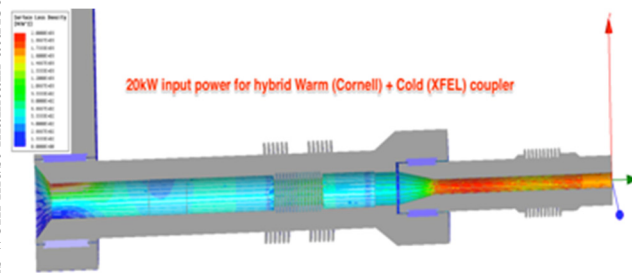


Figure 2: Hybrid coupler with warm Cornell type window associated with and cold XFEL type window.

As expected, the power loss density is higher in the hybrid coupler than the Cornell one, especially for the cold window which could be fully understood as the diameter size of the antenna and the inner warm/cold ceramic contact area were significantly decreased.

Coupling has also been simulated and optimized using a conditioning box and 2 different geometries for the coupler: Cornell-type coupler and hybrid coupler. The optimization has been done with 5 parameters: 3 parameters for the box size, one for the short circuit dimension and one for the antenna length. The short circuit size impacts on the coupling level and the antenna penetration shifts the peak in frequency in order to achieve 1.3 GHz, with S11 < -34 dB (see Fig. 3). At the moment no optimizations has been performed using the antenna shape, which would also impact the coupling.

THERMAL STUDIES

Thermal Analysis

The Fluent-HFSS coupling allows evaluating the RF losses in HFSS during the electromagnetic analysis and considering them in Fluent for thermal analysis. This link between the two solvers imports the EM field as heat flux (W/m²) on the inner/outer conductor and (W/m³) on the Warm/Cold window. This functionality is created in Workbench.

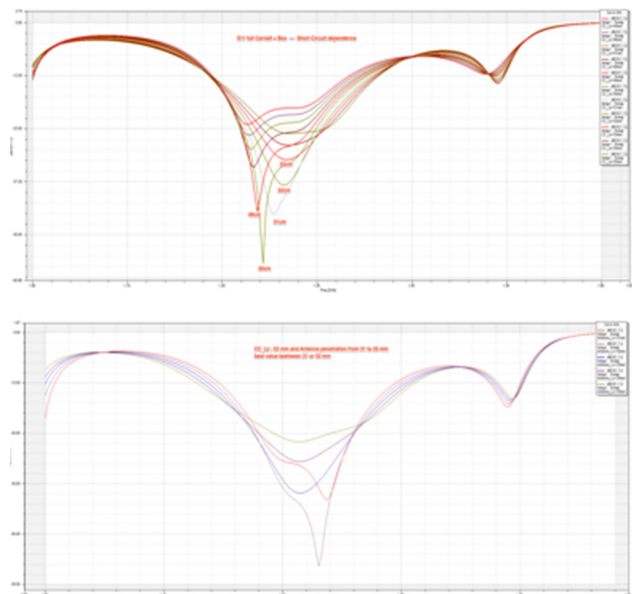


Figure 3: Coupling optimization: parameter S11 for different antenna penetration and short circuit length.

An initial evaluation using a two-dimensional thermal model of the coupler without cooling system shows that the temperature of the inner conductor can increase up to 450°C with input power equal to 225 W/m². This high temperature could generate heat radiation flux that disrupts the performance of the coupler. For this first part of the study, no cooling system is considered, except the outer conductors cooled by static air. We will limit the transmitted power to 3.7 kW CW in order to not exceed 230°C in the inner conductor.

For the numerical simulations, the parameters of thermal conductivities are taken as follows:

$$\lambda_{copper} = 420,75 - 6,8493 * 10^{-2} * T \quad (2)$$

Valid for 293<T<1300 (K),

$$\lambda_{steel} = 9,0109 + 1,5298 * 10^{-2} * T \quad (3)$$

Valid for 300<T<1000 (K),

$$\lambda_{Al2O3-ceramic} = 85,868 - 0,22972 * T + 2,607 * 10^{-4} * T^2 - 1,3607 * 10^{-7} * T^3 + 2,7092 * 10^{-11} * T^4 \quad (4)$$

Valid for 298<T<1600 (K).

Figure 4 presents the thermal conductivity dependencies with temperature variation for the different coupler materials.

The plots show that the copper and the ceramic thermal conductivities decrease with the temperature. While conversely, the stainless steel thermal conductivity increases proportionally to the temperature rise. Therefore, these variation tendencies will be taken into account in Fluent, this will be done using a polynomial function.

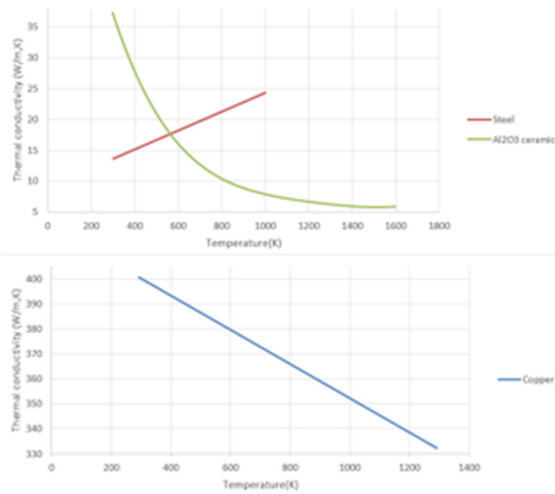


Figure 4: Thermal conductivity as a function of temperature for different materials constituting the coupler.

RF losses in the coupler operating at 3.7 kW CW are relatively high: Cold window (3.9W), Warm window (13.1W), Outer conductor (4.97W), Inner conductor (8.58W). Despite the limitation of the input power, these losses still critical and could produce irreversible damage in various elements of the coupler, in particular the windows, the most fragile coupler element.

The boundary conditions used for numerical simulation under ANSYS Fluent are: Surface energy loss in outer/inner conductor; Volumetric energy loss in warm/cold window; Outer conductor cooled by static air; Inner conductor cooled by radiation using temperature difference between the CX and CI.

The outer conductor cooling is taken into account on Fluent by defining different convective heat transfer coefficient values, which depend on the temperature and calculated using Nusselt number and Rayleigh number.

$$10^4 < Ra_D < 10^9: Nu_D = 0,53 * Ra_D^{\frac{1}{4}} \quad (5)$$

This correlation is used for vertical cylinder (same positioning of the power coupler during conditioning) with laminar airflow.

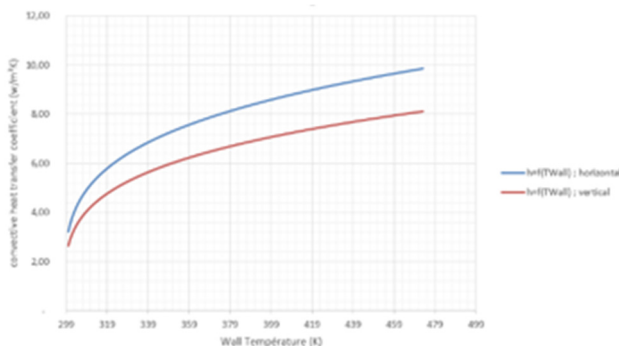


Figure 5: Convective heat transfer coefficient as a function of the outer conductor wall temperature.

In Fig. 5, we represent the convective heat transfer coefficient variation as function of outer conductor wall temperature for two coupler dispositions (horizontal and

vertical). These dependency is required as input for the accurate thermal simulations.

As shown on Fig. 6, the convective heat transfer coefficient depends on the coupler disposition. A vertical disposition as will be used during RF processing allow better convective heat transfer.

Simulation Results

The analytical thermal study does not allow a realistic description of the physical phenomena involved for two reasons: Firstly, the relatively complex 3D geometry of power coupler. Secondly, the strong dependencies on temperature of the couplers materials thermal properties. Thus, it is important to do a 3D thermal simulation.

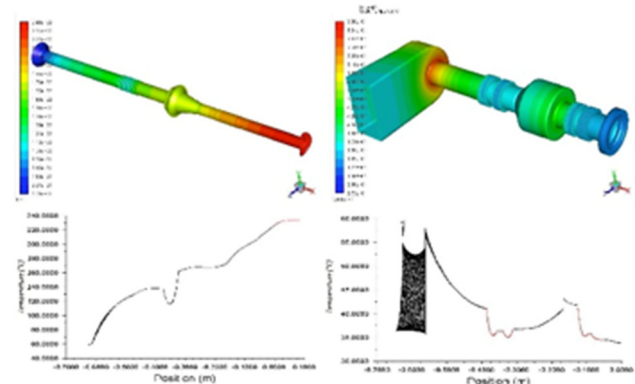


Figure 6: 3D simulation results of the power coupler.

The results above are valid for the following conditions:

- Room temperature 22°C
- Radiation emissivities: $\epsilon_{window}=0.8$ and $\epsilon_{CX/CI}=0.07$
- Input power equal to 3.7 kW.

For this power, the inner conductor (stands for the set inner warm-antenna in this case) temperature becomes high (230°C). As far as the other elements are concerned, the following Table 1 contain their maximum temperatures given that these temperatures are not homogenous.

Table 1: Different Elements Temperature

Power (CW)	T _{CI}	T _{CX}	T _{Cold-window}	T _{Warm-window}
3.7 kW	230°C	43°C	44°C	63°C

The Warm inner conductor temperature could be understood as the addition of two effects:

The top part of the warm inner conductor has a contact surface with the outer conductor. Thus, in addition to radiation, the heat transfer is also made by conduction. Therefore, more heat is evacuated to the outer conductor. this area of the coupler is characterized by temperature equal to 60 °C. The bellow located in the low part of the warm inner conductor has a very high thermal resistance (1,2 W/m.K) due to its length and thickness, so it tends to block the heat exchange from the warm to cold zone of the conductor which explains the observed increase of temperature in this area.

The overheating of the antenna is mainly due to the absence of any cooling system. Indeed, the principal way to evacuate its heat is by radiation.

Content from this work may be used under the terms of the CC BY 3.0 licence (© 2017). Any distribution of this work must maintain attribution to the author(s), title of the work, publisher, and DOI.

Emissivity Effect

A copper deposit with a thickness between 10 and 30(μm) is made on the inner/outer surface to reduce RF losses and increase its electrical conductivity. As a result, it's the copper emissivity that controls the heat evacuated and absorbed by radiation between the two conductors. The Table 2 below describes the temperature change as function of surface copper emissivity:

Table 2: Temperature Change as a Function of Emissivity

Copper quality	Emissivity	T _{CI} (°C)	T _{Cx} (°C)
Polished	0.02	370	40
Burnished	0.07	230	43
Oxidized	0.1	200	45

Table 2 shows a clear correlation between the inner and outer conductor temperature variation and the copper emissivity value. More the emissivity increases more the heat flux is evacuated from the inner to the outer conductor (the inner having the highest temperature). The increase of the outer conductor temperature is limited due to the fact that this later also exchange heat with the surrounding air.

A clear impact of the copper surface quality on the emissivity value is also shown in Table 2. Nevertheless, this parameter cannot be exploited as for power couplers, the usual copper surface finishing processes recommended (if any) are burnishing or glass bead blasting.

Equivalent Bellow Model:

The thickness of inner and outer bellows are respectively equal to: $e_{cx} = 0.2 \text{ mm}$; $e_{ci} = 0.12 \text{ mm}$. Those very small dimensions imply high mesh density on these areas. Therefore, approximately 60% of mesh elements on the power coupler are located on bellows. As a result, this requires considerable computing power and a long simulation time.

The most effective solution that can be deployed to considerably decrease mesh density is to use an equivalent bellows model. To do so, the bellows are replaced by copper (cu)/steel (ss) tube which has length “L” (bellow length at least), section “S” (thick tube section) and equivalent thermal conductivity “K_{eq}”.

$$K_{eq} = \frac{L}{d} \frac{S_{bellow}}{S} \frac{K_{cu} \cdot S_{cu} + K_{ss} \cdot S_{ss}}{S_t} \quad (6)$$

Figure 7 below shows the temperature behaviour for a bellow and its cylindrical equivalent model.

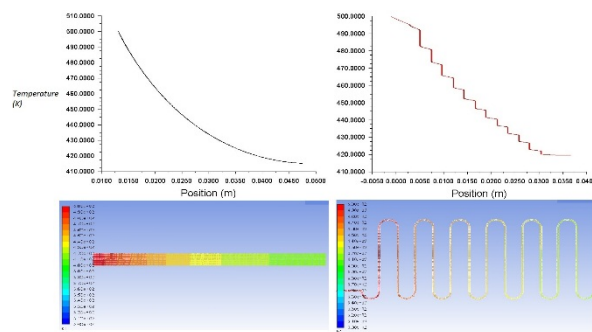


Figure 7: Equivalent bellows model validation.

The boundary conditions used to validate the equivalent bellows model are: convection cooling with static air and $T=500 \text{ K}$ at $x_{bellow}=0 \text{ mm}$. According to the simulation results, the temperature at $x_{bellow}=34 \text{ mm}$ is almost the same for the two cases and equal to 420 K for real bellow and 415 K for equivalent bellow. Which proves that the equivalent model is correct and can be used to reduce calculation time during the simulation.

CONCLUSION

1.3 GHz power coupler at 20kW CW maximum power is currently being designed at LAL-Orsay. Starting from the Cornell 62mm coupler design, EM and thermal studies are done using the HFSS software associated with Fluent inside Ansys Workbench. Hybrid coupler has also been considered with warm coupler part from the Cornell coupler and 40mm cold XFEL coupler part to fit to cavity connection constrain. Other alternative designs are under study. Further investigations are on going in particular concerning the cooling solutions. Principal concerns come from foreseen CW room temperature conditioning: indeed thermal simulations have shown that the maximum input power is about 4kW in CW, because of overheating along the cold antenna. In addition, as it is foreseen to perform a pulsed RF conditioning prior to CW one, we need to consider multipacting simulation study.

ACKNOWLEDGEMENT

Our warm thanks to the colleagues from the Cornell University for providing us with the mechanical folder of their 75kW CBETA injector power coupler.

REFERENCES

- [1] B. Dwersteg *et al.*, “TESLA RF power couplers development at DESY”, in *Proc. SRF'01*, Tsukuba, Japan, Sep. 2001, paper PT001, pp. 1-5.
- [2] V. Veshcherevich *et al.*, “Design of high power input coupler for Cornell ERL injector cavities”, in *Proc. SRF'97*, Ithaca, NY, USA, Oct. 1997, pp. 590-592.
- [3] S. Koscielniak *et al.*, “Ariel and the TRIUMF e-Linac initiative, a half MW electron Linac for rare isotope beam production”, in *Proc. LINAC'08*, Victoria, BC, Canada, Sep. 2008, paper TUP002, pp. 383-385.
- [4] A. Velez *et al.*, “BESSY VSR: A novel application of SRF for synchrotron light sources”, in *Proc. SRF'15*, Whistler, BC, Canada 2015, paper TUAA03, pp.462-466.